scientific reports

Check for updates

OPEN

Versatile high-power monolithic all-glass fiber amplifier for pulsed signals with a wide range of repetition rates

Hossein Fathi[1✉], Ebrahim Aghayari[2], Andrey Grishchenko[3], Amit Yadav[4], Edik Rafailov[4], Regina Gumenyuk[1,2] & Valery Filippov[2]

This study presents a compact, high-power monolithic all-glass spun tapered double-clad fiber amplifier for single-stage amplification of narrow linewidth picosecond pulsed signals from a few tens of mW to several hundred watts of average power and MW level of peak power, covering a wide range of repetition rates. The absence of free-space elements in the amplifier module enhances its overall reliability by omitting the dependency on the pump alignment and internal back reflections. The versatile all-glass amplifier module delivers 50 ps pulses with over 2 MW peak power at 1 MHz, 50 ps pulses with over 625 W average power at 20 MHz, and 20 ps pulses with over 645 W average power at 1 GHz, all exhibiting excellent spectral, spatial, and polarization characteristics. This monolithic all-glass ultra-large mode area fiber amplifier is verified as a robust solution for direct amplification of short pulses attaining high peak/average power laser systems with excellent spectral, spatial, and polarization characteristics.

Over the past two decades, significant progress was made in fiber laser technology, spurred by its outstanding properties. As a result, fiber lasers experienced remarkable advancements, further solidifying their importance across a wide range of laser-based applications, from scientific research to industrial processes. They emerged as a strong alternative to traditional laser sources due to their numerous inherent benefits, including superior beam quality and stability, high quantum efficiency, broad gain bandwidth, excellent thermal management, and turn-key operation[1]. Fiber lasers started slowly replacing traditional Ti:Sa lasers in the high-harmonic generation systems, offering higher repetition rates and low carrier-envelope phase noise. Providing sufficient average power scalability in combination with nonlinear post-compression, fiber-based laser systems are capable of keeping the required intensity level and transferring it to higher Extreme UV flux[2–4]. Furthermore, the amplification of high-repetition-rate (RR) pulses has gained significant interest in material processing for achieving both high-energy and high-peak-power pulses in kilowatt-class laser systems, particularly through burst-mode operation[5–8]. This approach allows for the simultaneous realization of highly intense pulses while maintaining manageable thermal loads in the laser system. By distributing energy over multiple bursts, the approach optimizes both power and performance, making it valuable for applications that require a balance between energy scaling and thermal management.

Amplifying short pulses directly within a single-stage fiber system poses challenges, primarily due to thermally induced transverse mode instabilities (TMI) and detrimental nonlinear effects such as stimulated Raman scattering (SRS). These issues are further compounded by a growing demand for compact and efficient short-pulsed amplifiers capable of delivering high-power/energy lasers while maintaining excellent beam quality, clean pulse profiles, and high polarization stability. Despite technological advancements, performance scaling in such systems remains fundamentally limited by TMI[9–12] and SRS[13], both of which can deteriorate spatial coherence and polarization properties[14,15].

One common approach to suppress SRS involves enlarging the core diameter and shortening the fiber length[1,16]. However, while effective for reducing nonlinear interactions, this method often reduces the TMI threshold, leading to unstable multimode operation and compromised beam quality. Therefore, achieving

[1]Laboratory of Photonics, Physics Unit, Faculty of Engineering and Natural Sciences, Tampere University, Korkeakoulunkatu 3, 33720 Tampere, Finland. [2]Ampliconyx Ltd, Lautakatonkatu 18, 33580 Tampere, Finland. [3]Ceramoptec SIA, Domes street 1a, LV-5316 Livani, Latvia. [4]Aston Institute of Photonic Technologies (AIPT), Aston University, Birmingham B4 7ET, UK. ✉email: hossein.fathi@tuni.fi

a practical trade-off between SRS mitigation and TMI suppression is essential for scaling high-power fiber systems[15,17]. To address this challenge, and simultaneously reduce the complexity of laser systems, Filippov et al. introduced the concept of tapered double-clad fibers (T-DCFs) in 2008[18]. T-DCFs are a specialized class of active double-clad fibers featuring a longitudinally increasing core and cladding diameter, formed by continuously adjusting the drawing speed during fabrication. The gradual increase in core size enables adiabatic mode field evolution, allowing the mode content to remain stable and consistent during amplification while the mode field area increases; this effectively raises the thresholds for nonlinear effects (NLEs). Compared to conventional double-clad fibers (DCFs), T-DCFs offer several key advantages: (1) higher thresholds for nonlinear effects due to increasing mode area, (2) improved pump absorption without requiring long fiber lengths, (3) preservation of beam quality and spatial coherence, and (4) suitability for compact, single-stage amplification without complex system architectures. Additionally, T-DCFs integrated with spun features deliver reliable polarization control over a broad range of power levels.

Besides nonlinear effects, polarization maintenance along the whole power range is another crucial aspect for high-power/energy laser systems. For T-DCFs, two primary approaches to maintaining the polarization state exist. The first involves introducing systematic strong birefringence into the fiber, which can be accomplished by incorporating stress rods, such as PANDA stress rods (so-called PT-DCF)[19]. The second approach minimizes intrinsic birefringence by spinning the fiber preform during the drawing process. This technique disperses the preform's non-uniformities in all directions, neglecting accumulated polarization errors as the signal propagates. This method, known as spun tapered double-clad fiber (sT-DCF), has been widely adopted to enhance polarization stability at high power levels[20,21]. Both PT-DCF and sT-DCF demonstrated strong amplification capabilities. The PT-DCF efficiently amplified low-power (mW) short-pulsed signals to high power and energy levels in a single amplifier stage with excellent beam parameters[22–26]. The sT-DCF achieved comparable performance, further highlighting its promise for efficient high-quality amplification[25,27]. The laser with a high peak power of 1.26 MW (10 W average power) was demonstrated using PT-DCF by A. Petrov in 2020[24], while for high average power, a level exceeding 573 W with $\sim$ 90% degree of linear polarization (DOP), and slope efficiency of 75% was achieved in sT-DCF without requiring additional pulse stretching techniques[25]. Notably, all implementations of T-DCF as the main amplifier were realized in a free-space pumping scheme, which required precise alignment to achieve high efficiency and control of heat dissipation, adding significant complexity to the setup and increasing the risk of damage. Recently, the design of completely monolithic T-DCFs using an all-fiber combiner was reported[28]. For a pulsed regime, this configuration involves the non-fusion fixing of a pump-feeding fiber on a wide side surface of the T-DCF, achieving a side-pumping record of 100 W[29].

In this paper, we report the amplification of various pulsed signals in a monolithic all-glass spun tapered double-clad fiber amplifier. The bulk elements-free, fully spliced configuration eliminates the alignment risk and enhances system robustness, enabling high-power operation in a compact and alignment-free architecture. Leveraging near-kilowatt pump powers, we achieve record-level performance across three distinct picosecond laser systems with different repetition rates: a 1 MHz system producing 50 ps pulses with over 2 MW peak power (155 W average power), a 20 MHz system achieving 50 ps pulses with up to 625 W average power (625 kW peak power), and a 1 GHz system generating 20 ps pulses with up to 645 W average power (32 kW peak power). These results surpass previously reported monolithic T-DCF-based systems, particularly in terms of average output power, polarization quality, and efficiency, all achieved without complex free-space coupling or bulk optics. Table 1 summarizes key results from the literature demonstrating optical pulse amplification using T-DCFs, including the performance achieved in this work. The demonstrated systems show excellent beam quality, high slope efficiency, and robust polarization stability across the full power range. Specifically, we achieve degrees of linear polarization (DOP) of 70%, 88.3%, and 87.6% for the 1 MHz, 20 MHz, and 1 GHz lasers, respectively. High peak power pulses exhibit beam quality of $M^2 \sim 2.0$ with slope efficiencies exceeding 59%, while high average power operation maintains near-diffraction-limited beam quality $M^2 < 1.36$ with slope efficiencies above 76%. Compared to previous implementations requiring free-space pumping or additional polarization-maintaining measures, our results demonstrate a clear advancement in terms of power scalability, system compactness, and beam integrity, establishing a new benchmark for monolithic all-glass fiber amplifier platforms suitable for short-pulse amplification across a wide range of repetition rates.

Ref.	Tapertype	Pump configuration	Average/peak power	Rep. rate	Pulse duration	Beam quality M^2
[27]	s-TDCF	Free space (counter-pump)	160 W/160 kW	20 MHz	50 ps	$M_X^2/M_Y^2 = 1.11/1.22$
[30]	PT-DCF	Free space (counter-pump)	13.8 W/1 MW	1.03 MHz	13 ps	$M_X^2/M_Y^2 \leq 1.2$
[24]	PT-DCF	Free space (counter-pump)	10 W/1.26 MW	100 kHz	48.8 ps	$M_X^2/M_Y^2 \simeq 1.3$
[26]	PT-DCF	Free space (counter-pump)	330 W/1.02 MW	10 MHz	35 ps	$M_X^2/M_Y^2 \leq 1.3$
[25]	PT-DCF sT-DCF	Free space (counter-pump)	457 W/457 kW 573 W/573 kW	20 MHz	50 ps	$M_X^2/M_Y^2 = 1.39/1.39$ $M_X^2/M_Y^2 = 1.38/1.31$
This work	sT-DCF	All fiber (bidirectional)	155 W/2 MW 625 W/625 kW 645 W/32 kW	1MHz 20 MHz 1 GHz	50 ps 50 ps 20 ps	$M_X^2/M_Y^2 = 2.0/2.0$ $M_X^2/M_Y^2 = 1.28/1.34$ $M_X^2/M_Y^2 = 1.36/1.36$

Table 1. Summary of reported pulsed MOPA systems using T-DCFs.

Experimental setup and results

Experimental setup

All amplifications of three different RR lasers were conducted using sT-DCF as the main amplifier in a master oscillator-power amplifier (MOPA) configuration. Figure 1 illustrates the schematic of the laser system consisting of three key parts: a front-end (F-E) seed laser system, sT-DCF as the main amplifier, and a pump unit. Despite the previous studies on sT-DCF where the pump was injected in free space using multiplexer assembly[19–21,24,25], this work employs monolithic all-glass sT-DCF-based amplifier, enabling alignment-free kW-pumping configuration.

The F-E seed laser system employs two seed laser sources: a tunable repetition rate gain-switched (GS) laser for delivering 50 ps pulses at repetition rates (RR) of 1 MHz and 20 MHz, and a mode-locked semiconductor (ML-SC) laser for generating 20 ps pulses at 1 GHz. The MHz F-E system consists of a 1040 nm GS laser diode with a polarization-maintaining (PM) fiber pigtail aligned along the slow axis, followed by two pre-amplifier stages. The GS laser output is amplified to over 5 mW and 100 mW at 1 MHz and 20 MHz, respectively, using two stages of PM core-pumped single-mode Yb-doped pre-amplifiers. To ensure stable operation, the F-E system incorporates a fiber in-line optical band-pass filter (BPF) centered at 1040 nm with a bandwidth of ±2 nm to suppress amplified spontaneous emission (ASE) from the pre-amplifiers. Additionally, an in-line fiber polarizer (ILP) is included to eliminate unwanted polarization states. Figure 2 depicts the optical spectra of MHz and GHz front-end laser systems. At 1 MHz RR, the signal-to-ASE ratio exceeds 20 dB (Fig. 2a), while at 20 MHz RR, it improves to more than 28 dB (Fig. 2b).

An ML-SC laser is used to efficiently generate 20 ps pulses at a 1 GHz repetition rate, meeting the rising demand for high-repetition-rate lasers, particularly in burst-mode laser systems. The high repetition rate reduces the pulse's peak power, simplifying the system by eliminating the need for pulse stretchers and enabling the implementation of more compact output compressors and solid-core delivery fibers. The ML-SC laser consists of a two-section chip (gain and absorber) integrated with an external cavity for efficient pulse generation. The laser is designed for high quantum efficiency (> 80%) and low series resistance with low internal optical losses. A layout of the layers for the laser is depicted in the GHz seed box in Fig. 1. The (In, Al) GaAs active region of the laser was grown using molecular beam epitaxy (MBE) by Innolume GmbH on the GaAs substrate. The active region of the laser consists of a single $In_xGa_{1-x}As$ quantum well (QW) layer to provide gain and desired wavelength. The QW layer is sandwiched between two layers of (In, Al) GaAs with the same composition to form an optical cavity in the vertical direction. This optical cavity is further sandwiched between AlGaAs cladding layers. These cladding layers support the growth of optical cavity layers by reducing stress due to lattice mismatch. Finally, a GaAs contact layer with p-type doping is grown on top to provide polarity to the laser diode and a minimal resistance platform for depositing the metal contacts. The external cavity length is calculated

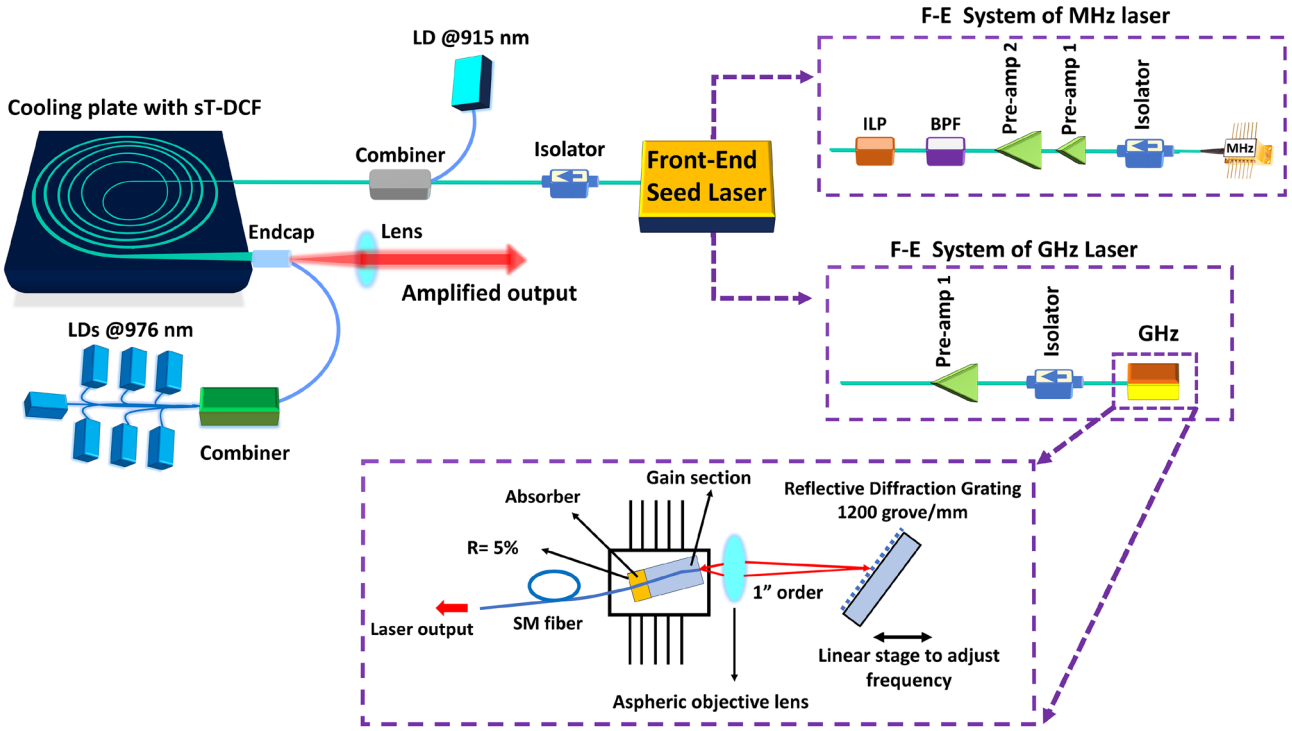

Fig. 1. Schematic of the experimental MOPA architecture using monolithic all-glass sT-DCF. The setup consists of three key parts: a front-end seed laser system, sT-DCF as a main amplifier, and a pump unit. The F-E seed laser system employs two seed laser sources: a tunable repetition rate GS laser for delivering 50 ps pulses at RR of 1 MHz and 20 MHz, and a ML-SC laser for generating 20 ps pulses at 1 GHz. The components are labeled as follows: Amp, amplifier; ISO, Isolator; BPF, bandpass filter; ILP, in-line polarizer; LD, laser diode.

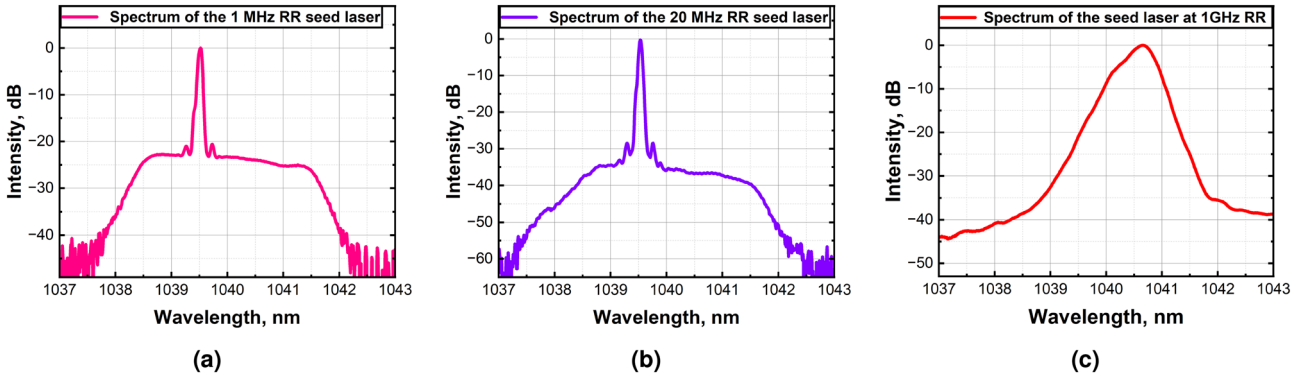

Fig. 2. Optical spectrum characterization of the MHz and GHz front-end laser system. (**a**) At 1 MHz repetition rate with 5 mW average output power, (**b**) at 20 MHz repetition rate with 100 mW average output power, (**c**) the optical spectrum of the 20 ps pulses of the 1 GHz mode-locked semiconductor seed laser with 120 mW average output power.

to correspond to $\sim$ 1 GHz pulse repetition rate in the ML regime. The semiconductor laser waveguide is split into two sections to form a saturable absorber section and a gain section, separated by a distance of a few micrometers. The total length of the 2-section semiconductor laser is 4 mm. A curved waveguide design is implemented to reduce back reflections in the external cavity configuration. The back facet on the curved end of the waveguide is coated with antireflection (AR) coatings that reflect < 0.001% of radiation. On the other hand, the straight section (front and the output) facet on the absorber side is coated with AR coatings to reflect $\sim$ 5% of radiation at laser wavelength around 1040 nm back into the cavity. The output of the laser is butt-coupled to the PM single-mode fiber. The external cavity of the laser is set up in the Littrow configuration. The output from the curved side of the waveguide was focused on a 1200 grooves/mm blaze reflective diffraction grating using an aspherical lens (f = 4.5 mm). The reflectivity of the grating at 1µm wavelength in the 1 st order is 80%. The grating is aligned to reflect the 1 st order into the gain section of the laser. Aligning the diffraction grating enables both wavelength tuning and stabilization of the laser, as well as adjustment of the repetition rate in the mode-locked regime. By carefully adjusting the grating, the laser is set to operate at 1040 nm with a 1 GHz pulse RR. Figure 2c depicts the optical spectrum of the 20 ps pulses of the 1 GHz mode-locked semiconductor seed laser (more than 40 dB of signal-to-noise ratio).

At the end of both the MHz and GHz F-E laser systems, a 10 W PM isolator protects the seed laser from high-power back reflections. This isolator has a minimum extinction ratio of 20 dB and a minimum isolation of 40 dB across all polarization states. The output of the F-E system was then spliced to the input signal port of a (2+1)$\times$ 1 combiner, which is pumped by an 18 W laser diode operating at 915 nm. The output port of the combiner is then spliced to the narrower side of the sT-DCF amplifier.

A spun Yb-doped tapered double-clad fiber is utilized as the main gain medium for the amplification of both MHz and GHz repetition rate laser systems. This fiber features two key attributes; tapering and spinning. Tapering is achieved through continuous adjustments in the drawing speed of the fiber preform, creating a conical shape of the fiber. However, the spinning is accomplished by rotating the preform at a specific angular velocity during the drawing process, which uniformly disperses preform non-uniformities in all directions and mitigates polarization errors as the signal propagates[21]. Consequently, the intrinsic internal birefringence is reduced to as low as $\approx 10^{-8}$, making the state of polarization (SOP) insensitive to heating caused by quantum defects[20,21]. Spinning the fiber affects the mode content and pump absorption. Therefore, optimizing the pitch length, core parameters, and cladding shape is crucial[21]. The sT-DCF utilized in this work has a constant spinning pitch length of 50 mm. The modified chemical vapor deposition (MCVD) technique was employed to manufacture the active core rod. The necessary thickness of the first cladding (pure silica) was created by sleeving with F300 silica tubes on a glass-working lathe. The fluorine-doped second cladding was deposited with the help of low-pressure microwave plasma[31]. Numerical Apertures (NA) for core/first cladding and first cladding/second cladding are 0,08 and 0,27 respectively. The cross-section of the first cladding was shaped to double D geometry to enhance absorption of pump irradiation. Glass of the sT-DCF was protected by a pair of acrylate coatings, where a low-index primary polymer creates an extra reflective layer with NA=0,48 relative to the first cladding. The taper exhibits an 800 dB/m core absorption at 976 nm. The diameters of the core, first clad, and second clad of the sT-DCF range from 8.3/75/90 μm to 90/814/977 μm over a length of $\approx$ 6.7 m length. The taper length, and particularly its profile, plays a critical role in determining the performance of the amplifier. It directly influences the effective interaction length within the fiber, thereby affecting the thresholds of nonlinear effects (NLEs), mode matching, and pump absorption efficiency. The taper length presents a design trade-off: a longer taper facilitates more efficient pump absorption and supports excellent beam quality through gradual mode adaptation. However, it also increases the interaction length, which can lower the threshold for effects such as Stimulated Brillouin Scattering (SBS). Therefore, optimizing the taper length and profile is essential to balance these competing factors, maximizing output power while maintaining spectral coherence and suppressing detrimental nonlinearities. Additionally, the sT-DCF features a double D-shape geometry on its first clad (pure silica glass) to enhance pump absorption and is protected by a low-index polymer coating. The

longitudinal profile of the active spun taper is illustrated in Fig. 3. The sT-DCF is coiled with a 35 cm diameter and positioned in the grooves of a water-cooled aluminium plate to ensure efficient heat dissipation. A 2-degree angled silica glass endcap (3 mm in diameter and 6 mm in length) is spliced to the wide end of the sT-DCF to eliminate back reflections and prevent potential damage from the high-power density at the air/silica interface. The amplifier's pump fiber is spliced to the endcap facet.

The main amplifier's pump unit comprises seven wavelength-stabilized laser diodes, each delivering up to 120 W of output power at 976 nm, providing a total output pump power of over 840 W. The output of the diodes is combined using a 7x1 fused-fiber pump combiner, which couples the pump light into a single fiber with a 200 μm core diameter. The output port of the combiner is then spliced to the pump fiber of sT-DCF, injecting the pump light into the wide side of the sT-DCF in a backward pump configuration. This alignment-free and integrated pumping scheme simplifies the system, reducing its complexity and making it more compact. The sT-DCF is predominantly pumped from the wide side using a 976 nm pump source, with an additional 18 W of power at 915 nm injected from the narrow side of the taper through a (2+1)×1 combiner. The use of 915 nm, despite its lower absorption cross-section compared to 976 nm, allows for a more gradual absorption along the fiber, helping to manage the uniform gain profile and reduce the onset of nonlinear effects such as SRS near the tapered fiber input, which can appear in case if the signal power grows fast. This dual-sided pumping scheme ensured optimal gain distribution and efficient energy transfer throughout the taper length, enabling the amplification of high-peak power pulses while maintaining a compact system architecture.

Amplification of 1 MHz laser

This section presents the amplification of 50 ps pulses at a 1 MHz repetition rate. The direct amplification of low repetition rates picosecond pulses is limited in standard constant core/clad ratio fibers due to the onset of strong nonlinear effects such as self-phase modulation and four-wave mixing, particularly at high power. However, T-DCFs offer a solution through their unique geometrical configurations to minimize nonlinear interactions and achieve high-power amplification. Using all-glass sT-DCF, a peak power of more than 2 MW (average power of 155 W) is achieved by direct amplification, with an optical efficiency of approximatly 59%. The peak power was determined by considering only the signal region, excluding the contribution of amplified spontaneous emission from the total output power. The dual-sided pumping strategy contributed to achieve the high peak powers while ensuring good energy transfer and gain distribution along the fiber. However, the fast growth of ASE and degradation of DOP limit further power scaling. Figure 4a depicts the average power at the laser system output as a function of the injected pump power. At maximum average output power (2 MW peak power), the system demonstrates around 70% of the degree of polarization (DOP), as shown in Fig. 4b. The polarization was measured over a 50-second interval using a commercial polarimeter (PAX1000IR2/M, Thorlabs). This assessment ensures the system maintains a reasonable polarization quality even at high peak power levels.

Figure 4c illustrates the optical spectra of the amplified signals across a narrow spectral range for different power levels. It shows that the 3 dB spectral bandwidth of the signal broadens slightly as the output power increases, from 0.45 nm at 3 W to 0.67 nm at 155 W. The optical spectra of the amplified signals across the wide wavelength range for different power levels are presented in Fig. 4d. The spectra reveal a 16.4 dB amplified spontaneous emission (ASE) background but no evidence of SRS, which typically poses a challenge in high-power fiber systems. However, the appearance of new spectral sidebands around 1020 nm and 1060 nm (signal at 1040 ± 20 nm), likely due to Polarization Modulation Instability (PMI)[32], highlights the impact of nonlinearities at elevated peak powers. These PMI-induced sidebands are generated by the coherent interaction of two polarization modes in a weakly birefringent optical fiber, potentially distorting the optical spectrum, degrading beam quality, and reducing overall system efficiency. To further verify the presence of PMI, we simultaneously measured the polarization directions of the emerging sidebands. The results showed that their polarization states

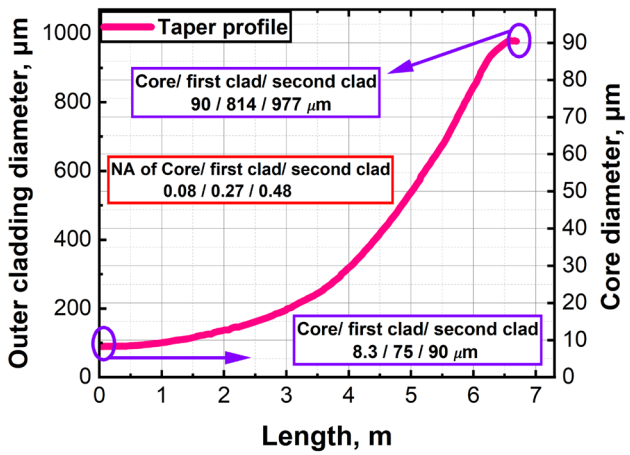

Fig. 3. Longitudinal profile of the active spun tapered double-clad fiber, illustrating the evolution of the core, first clad, and second clad diameters along the taper length.

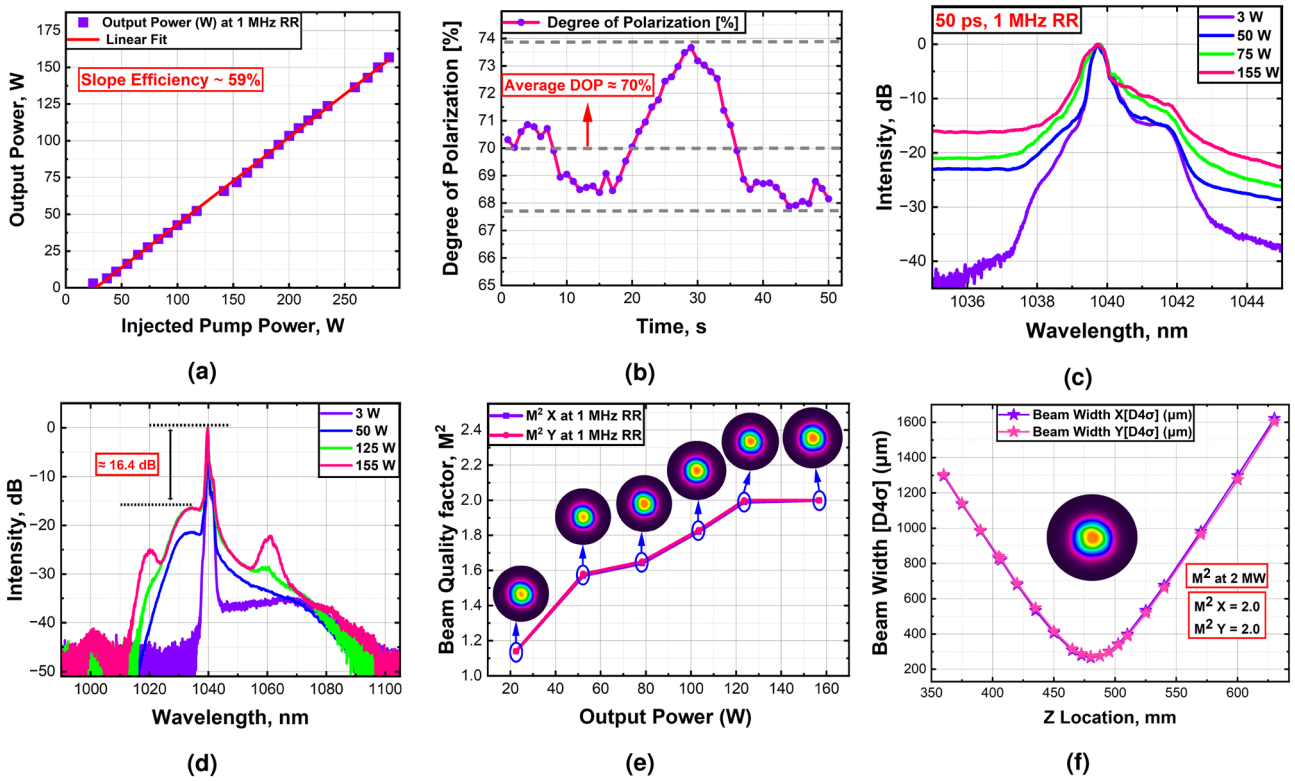

Fig. 4. Experimental characterization of the amplified 1 MHz pulsed signal. (**a**) The output power of the 1 MHz laser system versus the total launched pump power, showing the power scaling performance. (**b**) Degree of polarization measurements at the maximum output power. (**c**) and (**d**) represent the output optical spectrums at different output powers in narrow and wide spectral ranges, respectively. (**e**) The beam quality factor (M^2) measurements of the 1 MHz laser system at different output power alongside corresponding beam profiles. (**f**) Beam quality factor (M^2) measurement with beam profile inset at 2 MW peak power.

were nearly orthogonal in relation to the main signal polarization, which is a typical signature of PMI in weakly birefringent fibers.

In terms of beam quality, M^2 factor measurements provide valuable insights, see Fig. 4e and f. The measurements were carried out according to the ISO 11146 standard using the 4σ-method. Fig. 4e shows the evolution of beam quality with increasing output power, along with corresponding beam profiles. Notably, the intensity beam profile remained highly symmetric with a single intensity maximum across a wide range of operating conditions, even at maximum output power. At maximum power, the beam quality measured as $M^2X/M^2Y = 2.0/2.0$, indicating no sign of mode instability; see Fig. 4f (insets: near-field beam profile of the beam at 2 MW peak power). We attribute the increase in M^2 value with the output power growth mainly to the PMI effect and new wavelength generation at orthogonal polarization states.

The experimental results of amplifying high-peak-power pulses at a 1 MHz repetition rate via all-glass sT-DCF demonstrate effective amplification while maintaining good beam quality, high polarization stability, and manageable nonlinearities. The results mark a significant step toward scaling up short-pulse amplification in compact, high-power fiber laser systems.

Amplification of 20 MHz laser

This section presents the amplification of 50 ps pulses at a 20 MHz repetition rate in the all-glass sT-DCF amplifier module. Operating at full pump power, 625 W average output power is achieved with a slope efficiency of 76.6%. Further power scaling for the amplification of pulses was limited by the available pump power. Fig. 5a depicts the average output power versus the injected pump power. At the maximum output power of 625 watts, the degree of polarization was measured as 88.3%. This high degree of polarization signifies that the system successfully maintains a superior level of linear polarization even under the high thermal loads associated with maximum output power, see Fig. 5b. Figure 5c illustrates the optical spectra of the amplified signals across a narrow spectral range for different power levels. It shows that the 3 dB spectral bandwidth of the signal broadens slightly as the output power increases, from 0.38 nm at 20 W to 0.43 nm at 625 W. The optical spectra of the amplified signals across a wide spectrum range for different power levels are shown in Fig. 5d. The spectra demonstrate a low amplified spontaneous emission (ASE) background of $\approx$ 24.3 dB and a high signal-to-Raman peak suppression ratio of $\approx$ 45.7 dB, indicating efficient direct amplification of picosecond pulses.

Figure 5e, and f present the beam quality characterization of the 20 MHz laser system based on M^2 factor measurement. The evolution of the beam quality with increasing the output power, along with the corresponding

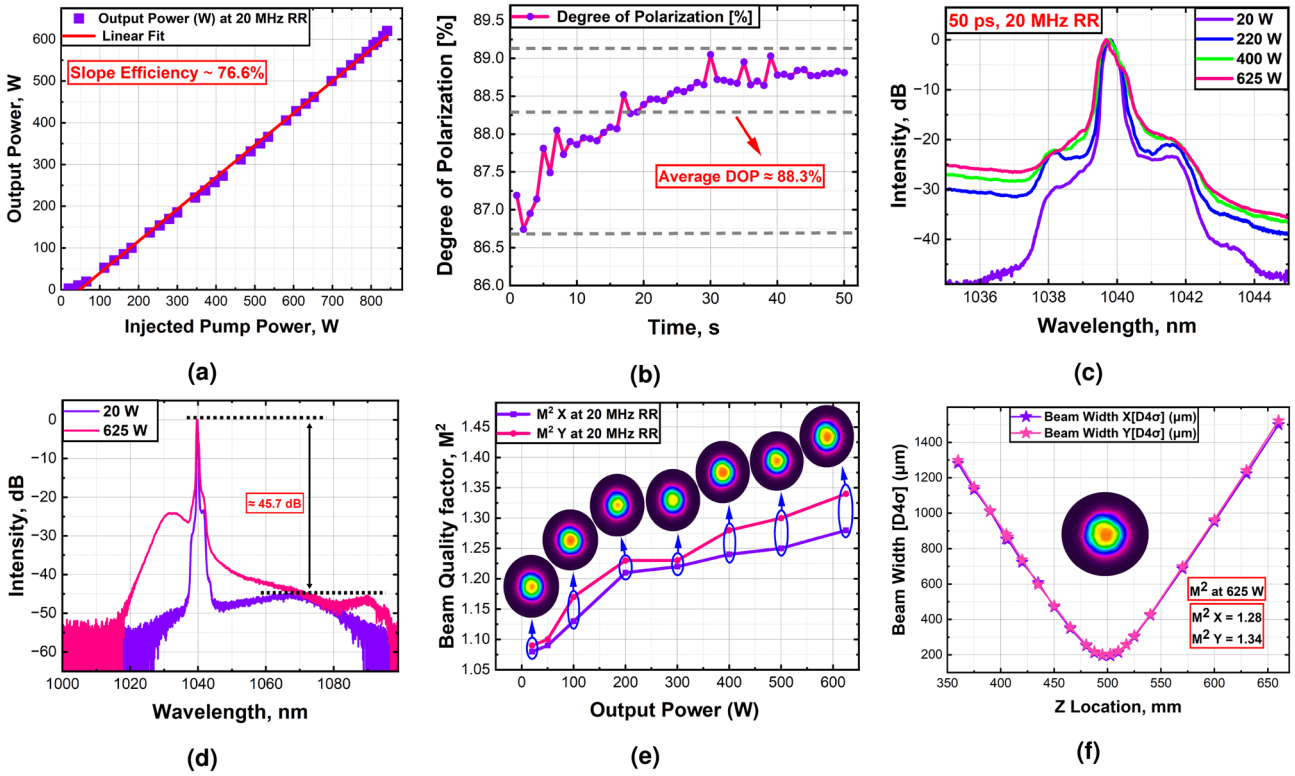

Fig. 5. Experimental characterization of the amplified 20 MHz pulsed signal. (**a**) The output power of the 20 MHz laser system versus the total launched pump power, showing the power scaling performance. (**b**) Degree of polarization measurements at the maximum output power. (**c**) and (**d**) represent the output optical spectrums at different output powers in narrow and wide spectral ranges, respectively. (**e**) The beam quality factor (M^2) measurements of 20 MHz laser system at different output power alongside corresponding beam profiles. (**f**) Beam quality factor (M^2) measurement with beam profile inset at 625 W average output power.

beam profiles, is depicted in Fig. 5e. At maximum power, the beam quality measured as $M^2X/M^2Y = 1.28/1.34$, indicating no sign of mode instability; see Fig. 5f (insets: near-field beam profile of the beam at 625 W average power).

Amplification of 1 GHz laser

This section reports on the successful amplification of 20 ps pulses at a high repetition rate of 1 GHz using an all-glass sT-DCF laser amplifier. The system achieved an average output power of 645 W with a slope efficiency of 78.6%. The available pump power ultimately limited further power scaling, as shown in Fig. 6a. Polarization measurements revealed a degree of polarization (DOP) of 87.6%, highlighting the system's ability to maintain excellent polarization quality even under high thermal loads at peak performance (Fig. 6b). Spectral analysis of the amplified signals across a narrow spectral range for different output powers is presented in Fig. 6c, showing a consistent 3 dB spectral bandwidth of around $\approx$ 0.51 nm, even at maximum output power. In addition, Fig. 6d displays the optical spectra of the amplified signals across a broad spectral range for different power levels. The spectra reveal $\approx$ 26.6 dB ASE background, but no evidence of SRS, which suggests the absence of significant Raman effects, indicating efficient direct amplification of picosecond pulses. Fig. 6e and f provide a characterization of the beam quality for the 1 GHz laser system based on M^2 factor measurement. The evolution of the beam quality with increasing the output power, along with the corresponding beam profiles, is depicted in Fig. 6e. This measurement shows that the intensity beam profile remains highly symmetric. At maximum power, the beam quality measured as $M^2X/M^2Y = 1.36/1.36$, indicating no sign of mode instability or degradation in beam shape; see Fig. 6f (insets: near-field beam profile of the beam at 645 W average power).

Discussion

In this report, we demonstrated the capability of all-glass sT-DCF for direct and efficient amplification of short-pulsed lasers with low input average power, maintaining a high degree of polarization and beam quality in a wide range of RR. The sT-DCFs featured ultra-large mode area, enabling amplification of a signal with a few tens mW average power up to 645 W average power or 2 MW peak power in a single-amplifier stage, preserving excellent single-beam propagation and linear polarization state simultaneously mitigating the SRS signal growth. The measurement results for amplifying three different RR laser systems, 1 MHz, 20 MHz, and 1 GHz are summarised in the Table 2. In the amplification of 50 ps pulses with 1 MHz RR, 155 W average output power was achieved with a slope efficiency of 59%. This corresponds to a remarkably high peak power of 2 MW. The maximum

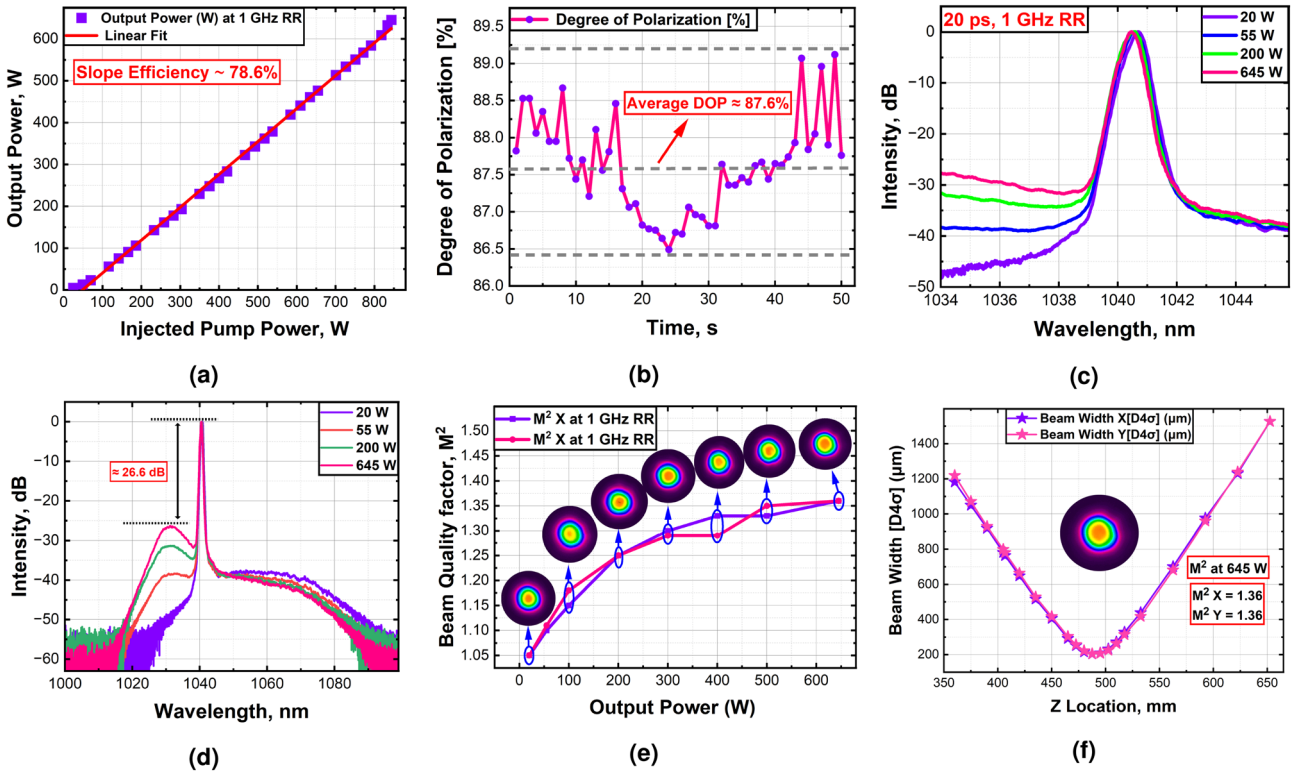

Fig. 6. Experimental characterization of the amplified 1 GHz laser system. (**a**) The output power of the 1 GHz laser system versus the total launched pump power, showing the power scaling performance. (**b**) Degree of polarization measurements at the maximum output power. (**c**) and (**d**) represent the output optical spectrums at different output powers in narrow and wide spectral ranges, respectively. (**e**) The beam quality factor (M^2) measurements of the 1 GHz laser system at different output power alongside corresponding beam profiles. (**f**) Beam quality factor (M^2) measurement with beam profile inset at 645 W average output power.

Properties	1 MHz RR, 50 ps	20 MHz RR, 50 ps	1 GHz RR, 20 ps
Taper length	6.7 m		
Diameters variation of core/first clad/second clad	8.3/75/90 μm to 90/814/977 μm		
NA of core/first clad/second clad	0.08/0.27/0.48		
Core absorption	800 dB/m		
Average/peak output power	155 W/2 MW (limited by ASE and DOP)	625 W/625 kW (limited by pump power)	645 W/32 kW (limited by pump power)
Slope efficiency	59%	76.6%	78.6%
Amplification gain	44.91 dB	39.82 dB	38.09 dB
Average of the DOP (at max output power)	70%	88.3%	87.6%
Signal-to-Raman ratio (at max output power)	No Raman signal	45.7 dB	No Raman signal
Signal-to-ASE ratio (at max output power)	16.4 dB	24.3 dB	26.6 dB
3 dB spectral bandwidth (at max output power)	0.67 nm	0.43 nm	0.51 nm
Beam Quality factor (at max output power)	$M_X^2/M_Y^2 = 2.0/2.0$	$M_X^2/M_Y^2 = 1.28/1.34$	$M_X^2/M_Y^2 = 1.36/1.36$

Table 2. Summary of experimental results for amplification of 1 MHz, 20 MHz, and 1 GHz seed lasers using the monolithic all-glass spun tapered double-clad fiber (sT-DCF).

power level was limited by the ASE and onset of DOP degradation, which we attributed mainly to the PMI effect appearing in the weakly birefringent fiber. By increasing the repetition rate of the GS seed laser from 1 MHz to 20 MHz, the same sT-DCF amplifier demonstrated higher efficiency and better maintenance of DOP, 76.6%, and 88.3%, respectively. The 3 dB spectral bandwidth was broader at 1 MHz compared to 20 MHz, measuring 0.67 nm and 0.43 nm, respectively. This difference was attributed to the higher levels of nonlinearity experienced during amplification at 1 MHz, where higher intensity per pulse leads to stronger nonlinear effects like self-phase modulation, resulting in greater spectral broadening compared to the repetition rate of 20 MHz. Moreover, the signal-to-ASE ratio at the maximum achieved power was higher at 20 MHz RR (24.3 dB) compared to 1

MHz RR (16.4 dB). This is attributed to more efficient population inversion depletion at higher repetition rates, which leads to less ASE build-up during amplification and thus results in a cleaner, higher-quality output signal. Further power scaling for the amplification of pulses at 20 MHz was limited by pump power. For amplification of high RR pulses, 20 ps pulses at 1 GHz RR were amplified up to 645 W, the highest average power achieved for narrow linewidth pulses using sT-DCFs to date. The amplification showed a high slope efficiency of 78.6%. Further power scaling for the amplification of pulses at 1 GHz was limited by the available pump power. The sT-DCF amplifier indicated a negligible Raman signal with a level 45.7 dB lower than the main signal peak, which appeared only in the amplification of a 20 MHz pulsed signal. Regarding the beam quality analysis, both the 20 MHz and 1 GHz lasers exhibited beam quality factors of $M^2 < 1.36$, indicating nearly diffraction-limited beam quality. In contrast, the 1 MHz laser showed a noticeably higher M^2 factor of 2, primarily due to nonlinear signal generation in orthogonal polarization states caused by the PMI effect. Although the M^2 factor of 2 typically indicates higher-order mode generation, the beam remained symmetrical, featuring a single intensity maximum without any visible spatial modulation effects. In addition to performance metrics, long-term operational stability was evaluated for all three repetition-rate systems. The laser systems were operated continuously at high power for approximately 5 hours, serving as a case study for long-term stability. During this period, power and polarization stability were monitored, and the system demonstrated stable operation throughout. Thermal stability was assessed using a thermal camera, which monitored the amplifier's housing and active regions. The temperature remained uniformly distributed across all components, with no evidence of localized overheating, indicating effective thermal management and confirming the robustness of the monolithic all-glass sT-DCF amplifier under sustained operation.

Conclusion

In conclusion, this study demonstrated a compact, high-power monolithic all-glass spun tapered double-clad fiber amplifier for direct amplification of narrow linewidth picosecond pulses from a few tens of mW to several hundreds of watts in a single-stage amplification, covering a wide range of repetition rates. The amplifier with a bulk elements-free configuration neglected the alignment failure of the nearly kW pump signal, leading to the better performance of the high-power laser system. The successful amplification of three different repetition rate pulsed signals in the all-glass sT-DCF-based amplifier was demonstrated: 1 MHz (50 ps) over 2 MW peak power, 20 MHz (50 ps) up to 625 W average power, and 1 GHz (20 ps) up to 645 W average power, exhibiting excellent spectral, spatial, and polarization characteristics. The system maintained a high degree of linear polarization at maximum power levels, achieving 70%, 88.3%, and 87.6% for the 1MHz, 20 MHz, and 1 GHz lasers, respectively. High peak power pulses exhibited beam quality of $M^2 \sim 2.0$ at the highest power level with a slope efficiency of exceeding 59%, while, high average power pulses exhibited near diffraction limited beam quality, $M^2 < 1.36$ at the highest average output power levels with a slope efficiency of more than 76%. These results represent significant advancements in narrow linewidth short pulsed laser amplifiers utilizing all-glass ultra-large mode area fiber with remarkable spatial and temporal characteristics and a high degree of polarization, which are suitable for further power/energy scaling of short pulses in a wide range of repetition rates.

Data availability

The datasets used and/or analyzed during the current study are available from the corresponding author on reasonable request.

Received: 23 December 2024; Accepted: 12 November 2025
Published online: 23 November 2025

References

1. Zervas, M. N. & Codemard, C. A. High power fiber lasers: A review. *IEEE J. Sel. Top. Quantum Electron.* **20**, 219–241. https://doi.org/10.1109/JSTQE.2014.2321279 (2014).
2. Raab, A.-K. et al. Multi-gigawatt peak power post-compression in a bulk multi-pass cell at a high repetition rate. *Opt. Lett.* **47**, 5084–5087. https://doi.org/10.1364/OL.463960 (2022).
3. Shestaev, E. et al. Carrier-envelope offset stable, coherently combined ytterbium-doped fiber CPA delivering 1 kW of average power. *Opt. Lett.* **45**, 6350–6353. https://doi.org/10.1364/OL.409410 (2020).
4. Shestaev, E. et al. High-power ytterbium-doped fiber laser delivering few-cycle, carrier-envelope phase-stable 100 μJ pulses at 100 kHz. *Opt. Lett.* **45**, 97–100. https://doi.org/10.1364/OL.45.000097 (2020).
5. Liu, Y. et al. $>$ 100 W GHz femtosecond burst mode all-fiber laser system at 1.0 μm. *Opt. Express* **28**, 13414–13422, 10.1364/OE.391515 (2020).
6. Liu, S. et al. High-energy and high-peak-power GHz burst-mode all-fiber laser with a uniform envelope and tunable intra-burst pulses. *High Power Laser Sci. Eng.* **11**, e81. https://doi.org/10.1017/hpl.2023.62 (2023).
7. Li, F. et al. High-power GHz burst-mode all-fiber laser system with sub 300 fs pulse duration. *Photonics* **11**, 10.3390/photonics11060570 (2024).
8. Xiu, H. et al. 1200-W all polarization-maintaining fiber GHz-femtosecond-pulse laser with good beam quality. *Opt. Express* **31**, 41940–41951. https://doi.org/10.1364/OE.506631 (2023).
9. Eidam, T. et al. Experimental observations of the threshold-like onset of mode instabilities in high power fiber amplifiers. *Opt. Express* **19**, 13218–13224. https://doi.org/10.1364/OE.19.013218 (2011).
10. Jauregui, C., Stihler, C. & Limpert, J. *Transverse mode instability. Adv. Opt. Photon.* **12**, 429–484. https://doi.org/10.1364/AOP.385184 (2020).
11. Zervas, M. N. Transverse mode instability, thermal lensing and power scaling in Yb^{3+}-doped high-power fiber amplifiers. *Opt. Express* **27**, 19019–19041. https://doi.org/10.1364/OE.27.019019 (2019).
12. Möller, F. et al. Polarization-resolved mode evolution in TMI-limited Yb-doped fiber amplifiers using a novel high-speed stokes polarimeter. *Opt. Express* **31**, 44486–44500. https://doi.org/10.1364/OE.505716 (2023).
13. Limpert, J. et al. High repetition rate gigawatt peak power fiber laser systems: Challenges, design, and experiment. *IEEE J. Sel. Top. Quantum Electron.* **15**, 159–169. https://doi.org/10.1109/JSTQE.2008.2010244 (2009).

14. Zeng, L. et al. Optimization and demonstration of 6 kW oscillating-amplifying integrated fiber laser employing spindle-shaped fiber to suppress SRS and TMI. *Opt. & Laser Technol.* **159**, no. 108903, 10.1016/j.optlastec.2022.108903 (2023).
15. Hejaz, K. et al. Modal instability induced by stimulated raman scattering in high-power Yb-doped fiber amplifiers. *Opt. Lett.* **42**, 5274–5277. https://doi.org/10.1364/OL.42.005274 (2017).
16. Stutzki, F. et al. Designing advanced very-large-mode-area fibers for power scaling of fiber-laser systems. *Optica* **1**, 233–242. https://doi.org/10.1364/OPTICA.1.000233 (2014).
17. Wang, L. et al. Origin of SRS-induced beam quality distortion under TMI threshold. *Opt. Express* **31**, 20237–20243. https://doi.org/10.1364/OE.480995 (2023).
18. Filippov, V. et al. Double clad tapered fiber for high power applications. *Opt. Express* **16**, 1929–1944. https://doi.org/10.1364/OE.16.001929 (2008).
19. Fedotov, A. et al. Ultra-large core birefringent Yb-doped tapered double clad fiber for high power amplifiers. *Opt. Express* **26**, 6581–6592. https://doi.org/10.1364/OE.26.006581 (2018).
20. Fedotov, A. et al. Active tapered double-clad fiber with low birefringence. *Opt. Express* **29**, 16506–16519. https://doi.org/10.1364/OE.421958 (2021).
21. Fedotov, A. et al. Large mode area double-clad ytterbium-doped spun tapered fiber. *J. Opt. Soc. Am. B* **38**, F161–F169. https://doi.org/10.1364/JOSAB.438013 (2021).
22. Kerttula, J., Filippov, V., Chamorovskii, Y., Golant, K. & Okhotnikov, O. G. Actively Q-switched 1.6-mJ tapered double-clad ytterbium-doped fiber laser. *Opt. Express* **18**, 18543–18549, 10.1364/OE.18.018543 (2010).
23. Patokoski, K. et al. Single-frequency 100 ns / 0.5 mJ laser pulses from all-fiber double clad ytterbium doped tapered fiber amplifier. *Opt. Express* **27**, 31532–31541, 10.1364/OE.27.031532 (2019).
24. Petrov, A. et al. Picosecond Yb-doped tapered fiber laser system with 1.26 MW peak power and 200 W average output power. *Sci. Reports* **10**, no. 17781, https://doi.org/10.1038/s41598-020-74895-z (2020).
25. Fathi, H. et al. Yb-doped tapered double-clad fibers with polarization maintenance for half-kW power amplifiers. *Opt. Express* **32**, 33064–33074. https://doi.org/10.1364/OE.533452 (2024).
26. Roy, V. et al. High-power/energy large mode area tapered fiber amplifiers. In Zervas, M. N. (ed.) *Fiber Lasers XVIII: Technology and Systems*, vol. 11665, 1166509, https://doi.org/10.1117/12.2584194. (International Society for Optics and Photonics, SPIE, 2021).
27. Kozlov, A. et al. Picosecond laser with Yb-doped tapered double clad fiber. In *2024 International Conference on Electrical Engineering and Photonics (EExPolytech)*, 464–467, https://doi.org/10.1109/EExPolytech62224.2024.10755578 (IEEE, 2024).
28. Bobkov, K. et al. Monolithic side-pumped amplifier based on an yb-doped tapered-fiber and yielding 0.53 MW 9.3 ps pulses. *Photonics* **9**, https://doi.org/10.3390/photonics9100771 (2022).
29. Mikhailov, E. K. et al. Scaling of average power in all-fiber side-pumped sub-MW peak power ps-pulses Yb-doped tapered amplifier. *Photonics* **11**, https://doi.org/10.3390/photonics11100915 (2024).
30. Mikhailov, E. K. et al. Picosecond pulse tapered fiber amplifier operated near 1030 nm with peak power up to 1 MW. *Photonics* **10**, https://doi.org/10.3390/photonics10121385 (2023).
31. Grishchenko, A. Effect of the preform fabrication process on the properties of all-silica optical fibres. *Quantum Electron.* **47**, 1115. https://doi.org/10.1070/QEL16550 (2017).
32. Murdoch, S. G., Leonhardt, R. & Harvey, J. D. Polarization modulation instability in weakly birefringent fibers. *Opt. Lett.* **20**, 866–868. https://doi.org/10.1364/OL.20.000866 (1995).

Acknowledgements

The authors thank Evgenii Motorin, Andrey Chumachenko, Konstantin Miroshnichenko, and Andrei Gurovich for their valuable contributions to this work. The authors would like to thank Prof. G. Genty for the valuable discussion about the PMI effect.

Author contributions

H.F. and E.A and R.G. and V.F. conceived the experiments. H.F. and E.A. conducted the experiments. H.F analyzed the results. A.G. supervised manufacturing of the main tapered amplifier. A.Y. and E.R. made the GHz seed laser. H.F. wrote the manuscript. All authors reviewed the manuscript.

Funding

Part of this work has been supported by the European Commission Horizon2020 program (PULSE project-grant agreement Nr. 824996) and the Flagship for Photonics Research and Innovation (PREIN).

Declarations

Competing interests

The authors declare no conflicts of interest.

Additional information

Correspondence and requests for materials should be addressed to H.F.

Reprints and permissions information is available at www.nature.com/reprints.

Publisher's note Springer Nature remains neutral with regard to jurisdictional claims in published maps and institutional affiliations.

Open Access This article is licensed under a Creative Commons Attribution 4.0 International License, which permits use, sharing, adaptation, distribution and reproduction in any medium or format, as long as you give appropriate credit to the original author(s) and the source, provide a link to the Creative Commons licence, and indicate if changes were made. The images or other third party material in this article are included in the article's Creative Commons licence, unless indicated otherwise in a credit line to the material. If material is not included in the article's Creative Commons licence and your intended use is not permitted by statutory regulation or exceeds the permitted use, you will need to obtain permission directly from the copyright holder. To view a copy of this licence, visit http://creativecommons.org/licenses/by/4.0/.

© The Author(s) 2025